

## NOTES AND CORRESPONDENCE

### Indian Monsoon Onset and the Americas Midsummer Drought: Out-of-Equilibrium Responses to Smooth Seasonal Forcing

BRIAN E. MAPES\*

*NOAA-CIRES Climate Diagnostics Center, Boulder, Colorado*

PING LIU

*International Pacific Research Center, University of Hawaii at Manoa, Honolulu, Hawaii*

NIKOLAUS BUENNING<sup>†</sup>

*NOAA-CIRES Climate Diagnostics Center, Boulder, Colorado*

(Manuscript received 9 April 2004, in final form 6 September 2004)

#### ABSTRACT

Two dominant high-frequency features of Northern Hemisphere summer climatology are examined in an atmosphere–land general circulation model (AGCM): the sudden onset of rains in south Asia, and the midsummer rainfall minimum in the tropical Americas. A control simulation succeeds in capturing these observed features fairly well. A slowed-calendar experiment is performed, to see whether these features are close to equilibrium with seasonally evolving forcings (orbital geometry and SST). The results indicate that some lag (disequilibrium) within the AGCM delays south Asian onset by about a month, from May in the experiment when seasonal forcing evolves extremely slowly to June in the normal, full-speed seasonal cycle. Disequilibrium also acts to delay and limit the amplitude of the Americas midsummer drought, and the associated intrusion of the Atlantic subtropical high into the Intra-Americas Seas' region. It is hypothesized that early summer (centered on the solstice) temperature over mid- and high-latitude continents, which differs greatly between experiment and control, drives the low-latitude rainfall differences. A more mysterious pole-to-pole, annual-mean, zonal wave-1 difference is also found in the slowed-calendar experiment.

#### 1. Introduction

The annual cycle is driven by top-of-atmosphere insolation with almost no amplitude at frequencies higher than semiannual (Fig. 1 of Mapes et al. 2004, manuscript submitted to *Bull. Amer. Meteor. Soc.*, hereafter MEA). The seasonal variation of sea surface tempera-

ture (SST) is also observed to be dominated by slowly varying Fourier components, away from regions of sea ice.<sup>1</sup> Prominent higher-frequency features of the mean annual cycle associated with Northern Hemisphere summer monsoons (known as singularities; e.g., Wang and Xu 1997) can therefore be deduced to arise from nonlinear internal dynamics of the land–atmosphere system. In addition to their real-world importance, these repeatable nonlinear phenomena pose clean challenges for climate models, in ways that may be relevant to other types of variations such as abrupt climate changes (e.g., deMenocal et al. 2000). Two such features are the famous sudden onset of the south Asian monsoon (Yin 1949; Wang and LinHo 2002) and a less studied subseasonal midsummer drought in the tropical Americas (Portig 1961; Magaña et al. 1999).

Various kinds of nonlinear dynamics could be involved. One possibility is that the land and atmosphere might be nearly in equilibrium with the slowly evolving seasonal cycles of SST and solar declination angle, but that this equilibrium response has an especially steep

<sup>1</sup> For example, the northern Arabian Sea has one of the biggest higher-frequency climatological variations of SST within the Tropics. This is dominated by the triannual (121 day period) harmonic, with an amplitude of only  $\sim 0.3$  K according to NCEP reanalysis data.

\* Current affiliation: Rosenstiel School of Marine and Atmospheric Sciences, University of Miami, Miami, Florida.

<sup>†</sup> Current affiliation: University of Colorado, Boulder, Colorado.

Corresponding author address: Brian Mapes, RSMAS, University of Miami, 4600 Rickenbacker Causeway, Miami, FL 33149.  
E-mail: bmapes@rsmas.miami.edu

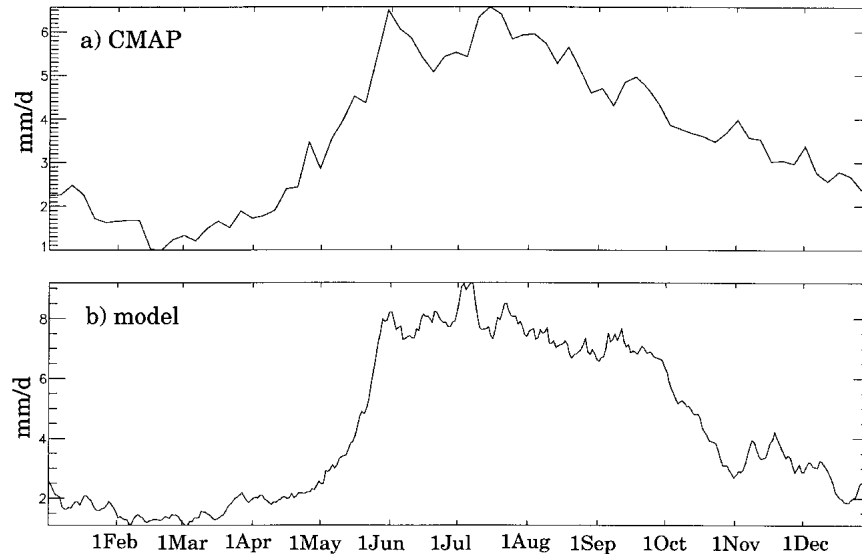


FIG. 1. Climatological mean rainfall rate in the Asian box shown in Fig. 3a. (a) CMAP observational estimate (Xie and Arkin 1997), 1979–2002, at pentad resolution. (b) The ECHAM/IPRC ACGM control run.

dependence on those forcings at certain times of year—for example, via the Clausius–Clapeyron equation’s nonlinear dependence of humidity on temperature. Another possibility is that the land and/or atmosphere have internal mechanisms characterized by subseasonal time scales, be they simple thermal-inertia lags or more complex mechanisms such as the soil moisture–precipitation feedback of Xie and Saiki (1999), set into motion as seasonal forcing crosses some instability threshold, such as the reversal of a meridional thermal gradient.

This note describes an experiment that bears on these different possible interpretations of monsoon singularities. If an atmosphere–land general circulation model (AGCM) were in equilibrium with solar and SST seasonality, then it would have the same mean climate on a given calendar date in both normal seasonal runs and in perpetual runs with the SST and solar angles fixed to their values on the date in question (e.g., Zwiers and Boer 1987). In this case, AGCMs could be used to isolate and explain singularities by examining differences between long perpetual-date runs on slightly different dates (as in Zhang and Held 1999). On the other hand, if monsoon singularities are out of equilibrium, perhaps in the form of Climatological Intraseasonal Oscillations (CISOs; Wang and Xu 1997), with explicit intraseasonal time scales arising within the atmosphere–land system but phase-locked to the calendar, then such a simple perpetual-date strategy could not succeed.

As a simple first step to assess the prospects for perpetual-date studies of monsoon singularities, we performed a pseudoperpetual, or slowed-calendar, experiment with an AGCM (model and strategy described in

section 2). Section 3 describes the dominant summertime differences, which indicate that the AGCM’s monsoons are significantly out of equilibrium with seasonal SST and solar forcings.

## 2. The model and its control-run monsoon singularities

The AGCM used here is a version of ECHAM-4 (Roeckner et al. 1996) running at the International Pacific Research Center (IPRC), where a dry adiabatic adjustment package has been added to suppress dry overturning in some tropical areas. The model is run at T42 horizontal resolution with 19 vertical hybrid layers, approximately 5 of which lie within the planetary boundary layer. The Tiedtke (1989) convection scheme, with a revised closure assumption and convective downdrafts proportional to updrafts, is used to represent deep, shallow, and midlevel convective activity. The prognostic cloud scheme is from Sundqvist (1978). Parameterized land-surface processes include soil-temperature profile evolution on five levels from 0.065- to 5.7-m depth, soil hydrology, and snowpack over land. Vegetation type and soil properties such as heat diffusivity, heat capacity, and water holding capacity are specified with spatially varying values. When snow depth exceeds a threshold of 0.025 m, the heat conduction equation is solved on an extra layer. More detailed description of the model and its modern climate simulation may be found in Roeckner et al. (1996).

The control run consisted of a 20-yr continuous integration with climatological SST seasonality. Output from the control run was averaged into a mean daily climatology, used for all results shown in this paper. This control run successfully simulates two observed

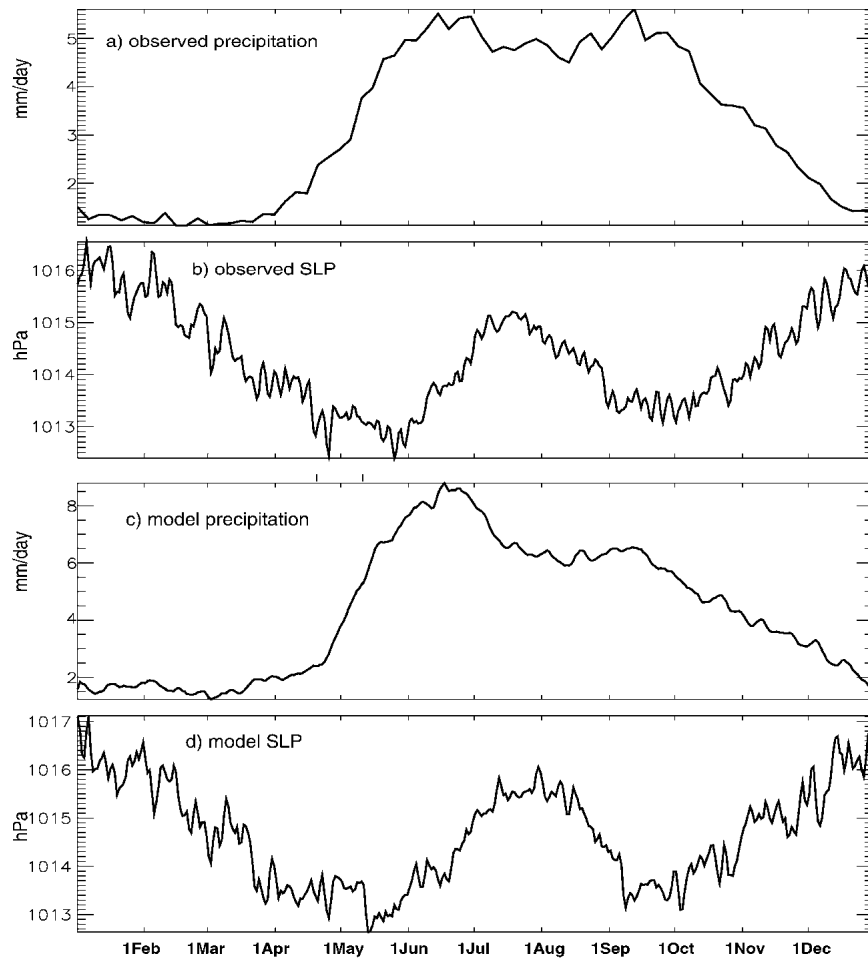


FIG. 2. (a),(b) Observed and (c),(d) simulated precipitation and SLP climatologies in the tropical Americas (approximately the box shown in Fig. 3a): (a) CMAP, 1979–2002; (b) SLP from NCEP–NCAR reanalysis, 1969–96; (c) and (d) from the AGCM control run.

monsoon singularities that are important to the model's response in the slowed-calendar experiment: the sudden Indian summer monsoon onset (ISMO) and the midsummer drought (MSD) in the northern tropical Americas.

The ISMO is shown in Fig. 1, in the form of observed (CMAP; Xie and Arkin 1997) and simulated time series of precipitation averaged over the south Asian box in Fig. 3a. In the Indian sector, a climatological belt of clouds and rain moves steadily northward during May–June in both observations and the AGCM (not shown), with the heaviest rains located over the northernmost Indian Ocean and commencing about 1 June. As a result, this regional-mean time series shows precipitation increasing strongly between about 1 May and 1 June, especially sharply in the model. The simulated and observed MSD in the Americas are indicated in Figs. 2a and 2c as time series of rainfall averaged over an area approximated by the other box in Fig. 3a.

In both observations and model, a midsummer sea level pressure (SLP) peak in the tropical Americas is also seen (Figs. 2b,d), corresponding to a midsummer strengthening and westward extension of the Atlantic subtropical high. Perhaps this affects rainfall through mechanisms discussed by Knaff (1997) for pressure anomalies on other time scales: “When pressures are anomalously high, subsidence is greater and middle levels are dryer. . .” The underlying cause would then lie in large-scale dynamics (discussed further in MEA), in contrast to the local air–sea interaction mechanisms offered by Magaña et al. (1999), in which the MSD (rainfall deficit) was suggested to be a response of the atmosphere to local subseasonal SST variations. Examination of reanalysis SST data in the region shows these subseasonal variations to be fairly small in amplitude and spatial coverage, and hence perhaps unlikely to be the primary or ultimate cause of the MSD. Model experiments with time-filtered SST data could clarify their importance, but are beyond the present scope.

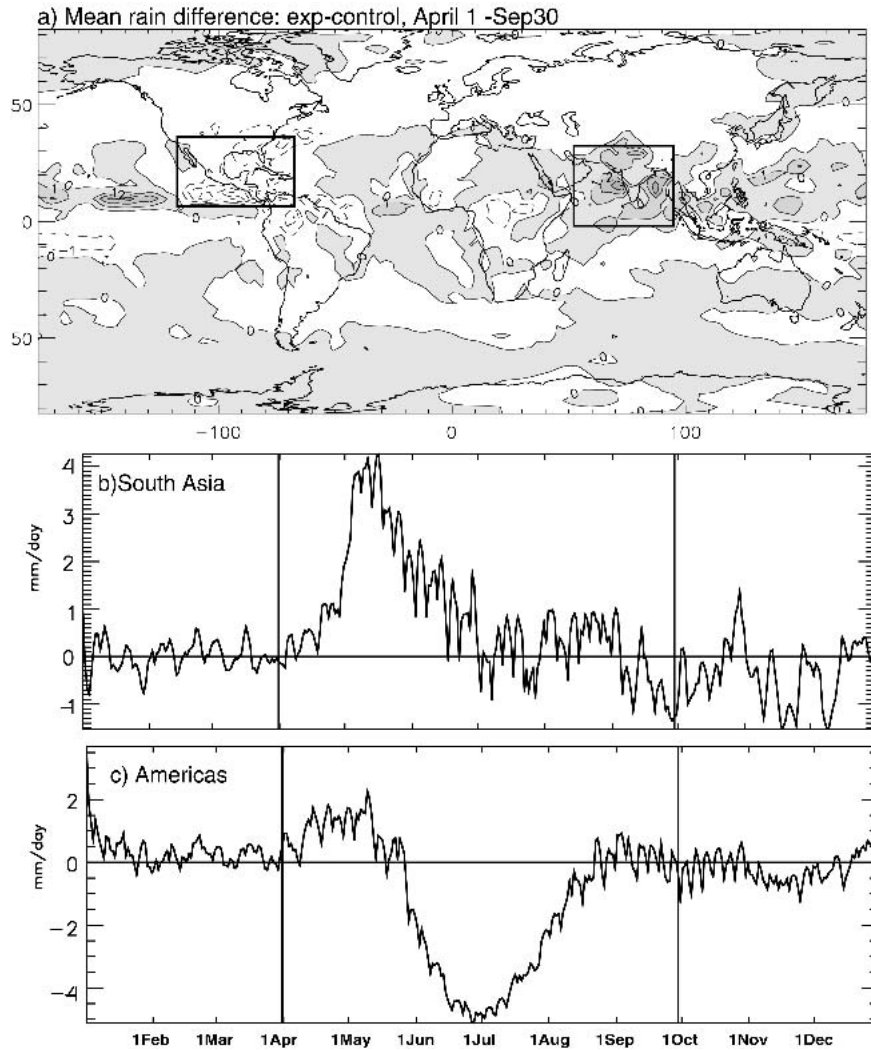


FIG. 3. (a) Mean rain-rate difference, experiment minus control, averaged over Apr–Sep. Contour interval 1 mm day<sup>-1</sup>; positive areas shaded. (b) Time series of the experiment minus control over the south Asian box indicated in (a). (c) As in (b), but for the Americas box (where 5-day smoothing misses the end points, enlarging the coincidental spike near 1 Jan).

### 3. Experimental results

The experimental slowed-calendar run, motivated in section 1, consisted of a continuous  $20 \times 365$  day integration of the model, but with the SST and solar declination angle fixed at their value on each calendar date for 5 days. That is, 1 January SST and solar angle were maintained for 5 days, then 2 January, and so on, while the atmosphere and land model responded continuously. Since 5 days is not forever, we call this strategy *pseudoperpetual*. The cycle of pseudoperpetual dates was repeated 4 times, and daily output data were averaged into a 365-pentad climatology, with each pentad mean corresponding to a calendar date. The figures here present differences, experiment minus control, be-

tween the 365-pentad slowed-calendar and 365-day normal mean annual cycles.

The experiment–control difference in rainfall averaged over April–September is shown in Fig. 3. The south Asian region experiences increased rainfall, with the absolute differences greatest over the northern Indian Ocean, where mean monsoon rainfall is already most abundant (not shown). Meanwhile the Americas experience drier summers in the slowed-calendar experiment, throughout the Tropics and subtropics, with some apparently compensatory rainfall increases along 10°N, 120°–150°W.

In south Asia, the time series of rainfall difference (Fig. 3b) shows that an earlier onset of the rains is the dominant effect: summer rains in the northern Indian

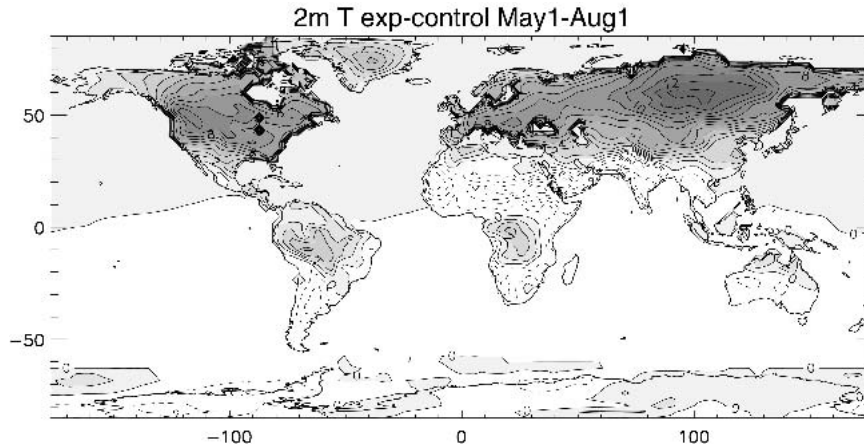


FIG. 4. May–Jul mean differences in near-surface air temperature, experiment minus control. Contour interval 1 K; positive areas shaded.

ocean region begin near 1 May in the experiment, rather than near 1 June as in the control run (Fig. 1b), but have very similar mean intensity through the middle and late summer. Stated as a finding about the control run, the results indicate that a lag of about 1 month in the atmosphere–land system acts to delay the onset of monsoonal rains over south Asia, from about May, when boundary conditions can (if sustained) allow it, to around 1 June. Mechanisms for a  $\sim 1$  month lag include atmospheric thermal inertia (North and Coakley 1979; Zhang and Held 1999) or land effects. A similar lag was found by Xie and Saiki (1999), who emphasized soil moisture mechanisms but noted that two-dimensional aspects of atmospheric adjustment can have time scales approaching a month (Plumb and Hou 1992).

In contrast, the tropical Americas have drier summers in the experiment, because of a drier midsummer season centered on about 1 July (Fig. 3c). Comparing with Fig. 2c, this is seen to correspond to an earlier as well as drier MSD. A modest increase is seen in the month centered around 1 May, as in south Asia, but the MSD dominates the seasonal mean.

To better interpret these rainfall differences, consider the basic hemispheric and continental-scale thermal forcing for the monsoons. Figure 4 shows a map of the summertime (May–July) mean temperature difference in the slowed-calendar experiment. Northern middle and high latitude continents have much hotter summers, with maximum differences near  $50^{\circ}$ – $60^{\circ}$ N, almost 15 K in Siberia and up to 10 K in North America. These thermal anomalies are centered almost exactly on the June solstice (not shown), consistent with the interpretation of the slowed-calendar run as having the land–atmosphere system nearer to equilibrium with solar forcing. The lengthened summer may also dry out the land surface, tilting the Bowen ratio toward increased sensible heat fluxes and hotter weather. Over

India and southeast Asia, May is cooler, owing to the early onset of clouds and rain seen in Fig. 3b. The Sahara–Arabia region is also cooler in northern summer, but this is merely a modest enhancement of a year-round difference, associated with low-latitude westerly wind increases in an annual mean planetary-scale, low-level circulation (Fig. 5). We do not understand the origins of this pole-to-pole, zonal wave-1 difference.

Returning to the Americas midsummer drought, the map of May–July experiment–control SLP difference in the region is shown in Fig. 6. Pressure increases are seen across the subtropical latitudes, with a local maximum in the Gulf of Mexico. Although mountains complicate the SLP picture somewhat in the west, there is a negative pattern correlation between temperature (Fig. 4) and SLP, both on the continental scale (as the much hotter northern United States and Canada have lower pressure), and on smaller scales (with local maxima over the relatively cooler prescribed water temperatures of the Gulf of Mexico and Hudson’s Bay). These patterns in the experiment–control difference lead us to hypothesize that the midsummer westward extension of the Atlantic High (Fig. 2b,d; see MEA for maps) in the mean climate may be significantly shaped by land–ocean thermal contrasts in the Intra-Americas Seas region. Nonetheless, planetary-scale dynamics (as glimpsed in Fig. 5) are also clearly important, with the Atlantic–Americas sector strongly affected by the powerful Asian monsoon (cf. Chen et al. 2001; Rodwell and Hoskins 2001).

#### 4. Conclusions

In summary, the AGCM used here simulates two prominent Northern Hemisphere summer monsoon singularities well: the sudden Indian summer monsoon

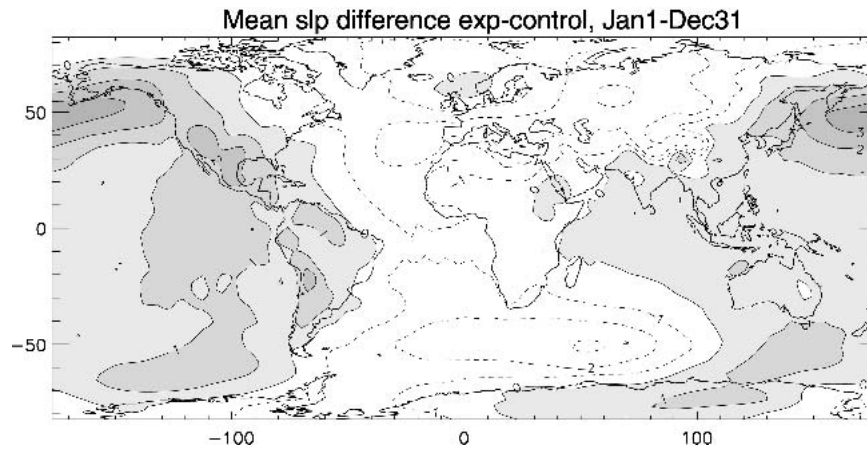


FIG. 5. Annual mean SLP difference, experiment minus control. Contour interval 1 hPa; positive areas shaded.

onset (ISMO), and the midsummer drought (MSD) of the tropical Americas. To explore whether these singularities are sufficiently in equilibrium with seasonal boundary conditions to allow study using perpetual-date runs, a pseudoperpetual or slowed-calendar experiment was performed. July results are all broadly similar to those of Zwiers and Boer (1987).

In the longer summer, Eurasia gets hotter, with the difference rising steadily after April 1 and peaking near the June solstice. This earlier heating-up of the continent causes ISMO to come about a month earlier. Correspondingly, the Asian monsoon low-pressure center becomes deeper through the summer season. Compensating pressure rises are concentrated in the Pacific sector, contributing to an east–west planetary wavenumber-1 pattern that persists throughout the year, and spans both southern and northern hemispheres. In the tropical Americas, the MSD and coincident midsummer intrusion of the Atlantic high into the IntraAmeri-

cas Seas are intensified in the slowed-calendar experiment. This undercutting-high spatial pattern of the SLP field is also enhanced by pressure decreases over the hotter middle and high latitudes of North America.

These findings re-emphasize the importance of land temperatures in determining the monsoonal climate of the AGCM. A time lag of about 1 month apparently characterizes the disequilibrium of the land–atmosphere system, similar to the  $\sim 1$  month lag of the annual harmonic of temperature over the northern continents behind the solstices (e.g., Trenberth 1983). The fact that the model simulates monsoon singularities in the control run (Figs. 1,2) suggests that it is a useful tool for understanding the dynamics of monsoon singularities or climatological intraseasonal oscillations, but methods other than perpetual-date runs will be necessary. Knowledgeable diagnoses and appropriate control strategies for model land-surface processes will be important to such future work.

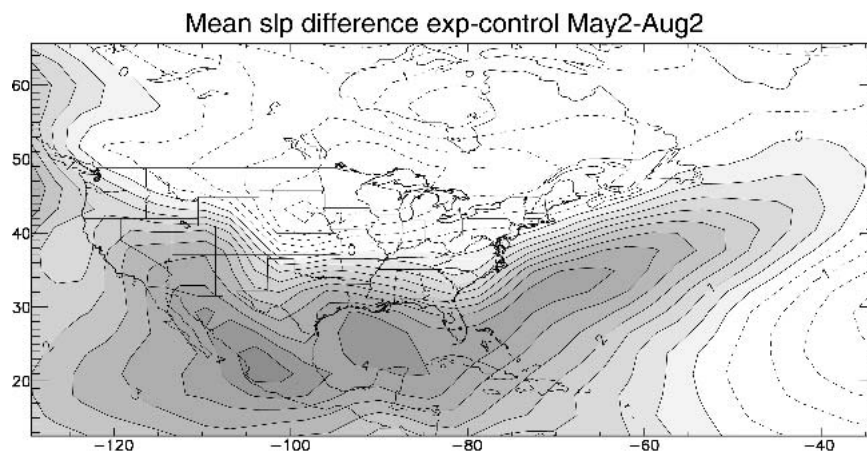


FIG. 6. May–Jul mean SLP difference, experiment minus control. Contour interval 1 hPa; positive areas shaded.

*Acknowledgments.* This research was supported by National Science Foundation Grants ATM-0073206 and ATM-0112715, and by a PACS-GAPP grant from the NOAA Office of Global Programs. Constructive comments from two anonymous reviewers were very helpful.

## REFERENCES

- Chen, P., M. P. Hoerling, and R. M. Dole, 2001: The origin of the subtropical anticyclones. *J. Atmos. Sci.*, **58**, 1827–1835.
- deMenocal, P. B., J. Ortiz, T. Guilderson, J. Adkins, M. Sarnthein, L. Baker, and M. Yarusinsky, 2000: Abrupt onset and termination of the African Humid Period: Rapid climate responses to gradual insolation forcing. *Quat. Sci. Rev.*, **19**, 347–361.
- Knaff, J. A., 1997: Implications of summertime sea level pressure anomalies in the tropical Atlantic region. *J. Climate*, **10**, 789–804.
- Magaña, V., J. A. Amador, and S. Medina, 1999: The mid-summer drought over Mexico and Central America. *J. Climate*, **12**, 1577–1588.
- North, G. R., and J. A. Coakley Jr., 1979: Differences between seasonal and mean annual energy balance model calculations of climate and climate sensitivity. *J. Atmos. Sci.*, **36**, 1189–1204.
- Plumb, R. A., and A. Y. Hou, 1992: The response of a zonally symmetric atmosphere to subtropical thermal forcing. *J. Atmos. Sci.*, **49**, 1790–1799.
- Portig, W. H., 1961: Some climatological data of Salvador, Central America. *Weather*, **16**, 103–112.
- Rodwell, M. J., and B. J. Hoskins, 2001: Subtropical anticyclones and summer monsoons. *J. Climate*, **14**, 3192–3211.
- Roeckner, E., and Coauthors, 1996: The atmospheric general circulation model ECHAM-4: Model description and simulation of present-day climate. Max-Planck-Institut für Meteorologie Rep. 218, 90 pp.
- Sundqvist, J. M., 1978: A parameterization scheme for non-convective condensation including prediction of cloud water content. *Quart. J. Roy. Meteor. Soc.*, **104**, 677–690.
- Tiedtke, M., 1989: A comprehensive mass flux scheme for cumulus parameterization in large-scale models. *Mon. Wea. Rev.*, **117**, 1779–1800.
- Trenberth, K. E., 1983: What are the seasons? *Bull. Amer. Meteor. Soc.*, **64**, 1276–1277.
- Wang, B., and X. Xu, 1997: Northern Hemisphere summer monsoon singularities and climatological intraseasonal oscillation. *J. Climate*, **10**, 1071–1085.
- , and LinHo, 2002: Rainy season of the Asian–Pacific summer monsoon. *J. Climate*, **15**, 386–398.
- Xie, P., and P. A. Arkin, 1997: Global precipitation: A 17-year monthly analysis based on gauge observations, satellite estimates, and numerical model outputs. *Bull. Amer. Meteor. Soc.*, **78**, 2539–2558.
- Xie, S.-P., and N. Saiki, 1999: Abrupt onset and slow seasonal evolution of summer monsoon in an idealized GCM simulation. *J. Meteor. Soc. Japan*, **77**, 949–968.
- Yin, M. T., 1949: A synoptic-aerologic study of the onset of the summer monsoon over India and Burma. *J. Meteor.*, **6**, 393–400.
- Zhang, Y., and I. M. Held, 1999: A linear stochastic model of a GCM's midlatitude storm tracks. *J. Atmos. Sci.*, **56**, 3416–3435.
- Zwiers, F. W., and G. J. Boer, 1987: A comparison of climates simulated by a general circulation model when run in the annual cycle and perpetual modes. *Mon. Wea. Rev.*, **115**, 2626–2644.